Precambrian Research 180 (2010) 227–236

Contents lists available at ScienceDirect

Precambrian Research

journal homepage: www.elsevier.com/locate/precamres

Episodic zircon age spectra of orogenic granitoids: The supercontinent connection and continental growth

Kent C. Condie*, Richard C. Aster

Department of Earth and Environmental Science, New Mexico Institute of Mining and Technology, Socorro, NM 87801, USA

ARTICLE INFO

Article history:
Received 30 October 2009
Received in revised form 18 March 2010
Accepted 31 March 2010

Keywords:
Zircon ages
Crustal evolution
Continental growth
Orogeny
Episodic ages

ABSTRACT

To identify age peaks and other features in an isotopic age distribution, it is common to perform a kernel density estimation or similar analysis. A key aspect of this estimation process is the choice of an age resolution bandwidth that best reflects the random variable and other assumptions on the data. Probabilistic kernel density analysis of large databases (up to nearly 40,000 samples) of U/Pb zircon ages suggests an optimum bandwidth of 25–30 My for many key features, which yields approximately 40 peaks with confidence levels of $c \geq 0.9$. Because of natural redistribution processes, geographic sample bias may be minimized by jointly analyzing isotopic ages from both orogenic granitoids and from detrital zircons. We show that the relative heights of age peaks are commonly controlled by the local geographic distribution of samples and are not necessarily correlated with total geographic extent. Eight peaks with $c \geq 0.9$ occur on five or more cratons or orogens (at 750, 850, 1760, 1870, 2100, 2650, 2700, and 2930 Ma). Results suggest that orogenic plutonism age peaks principally reflect subduction system episodicity on local or regional scales, but not on continental or supercontinental scales. In contrast, peak clusters that are jointly defined by granitoid and detrital ages may be more representative of the general age distribution of the continental crustal record.

Five major peak clusters are closely tied to supercontinent formation at 2700, 1870, 1000, 600, and 300 Ma and minima in age spectra correspond to supercontinent stasis or breakup (2200–2100, 1300–1200, 750–650, and ≤200 Ma). Age clusters also show a decrease in cycle duration beginning at 1000 Ma. A new histogram of continental preservation rate shows that approximately one-third of the extant continental crust formed during the Archean, about 20% during the Paleoproterozoic, and only 14% during the last 400 My. Peak clusters are probably related chiefly to preservation of juvenile crust in orogens during supercontinent assembly, although locally, continental crustal production rate may be enhanced during actual collisions.

1. Introduction

The episodic nature of terrestrial magmatism is widely recognized, but only in the last few years has it been well documented by high-precision U/Pb and Hf isotopic studies of zircons (Rino et al., 2008; Pietranik et al., 2008; Condie et al., 2009a; Wang et al., 2009a,b; Yang et al., 2009). Yet we still face two major interpretive problems: robust statistical estimation and identification of age peaks and troughs, and the geographic extent of peaks and troughs. Published age spectra commonly use histograms or density probability estimates. In such analyses, the age bandwidth used in smoothing data controls the tradeoff between resolution and statistical robustness of spectral features. Age peaks occurring on several different continents are often interpreted as global events, yet the term "global" is ambiguous because of sampling and preservation biases. For rocks older than 100 Ma almost all age data come from the continents, yet continents have never covered the complete surface of the Earth. For this reason, we avoid the term "global" for the ages of continental magmatism, and refer to geographic distributions as local, regional, or widespread on the continents based on the best presently available data.

Here, we analyze a large database of concordant and near-concordant U/Pb zircon ages (8928 igneous and 28,027 detrital ages) using combined Monte Carlo simulations and kernel density analysis with varying bandwidths to explore the optimal resolution and statistical inferences permitted by the data (e.g., Rudge, 2008). A summary of the U/Pb ages is given in Appendix 1. The age database of single zircon ages with uncertainties (with minor updates for this paper) is given in Condie et al. (2009a), and the $\varepsilon_{Nd}(T)$ data for whole rocks from which the zircon ages were determined are given in Condie et al. (2009b). Although most of the igneous data are high-precision TIMS (thermal ionization mass spectrometry) results, most of the detrital ages are from lower precision SHRIMP (sensitive high-resolution ion microprobe) and LAM ICP-MS (laser

* Corresponding author. Tel.: +1 505 835 5531; fax: +1 505 835 6436.
E-mail address: kcondie@nmt.edu (K.C. Condie).

0301-9268/$ – see front matter © 2010 Elsevier B.V. All rights reserved.
doi:10.1016/j.precamres.2010.03.008

ablation microprobe inductively coupled plasma mass spectrometry). From these results, we discuss the identification of age peaks and age peak clusters, possible geographic biases, and the significance of U/Pb age distributions in terms of the supercontinent cycle. This paper expands on Condie et al. (2009a,b) in that it introduces a new statistical method to identify meaningful age peaks, discusses the interpretation of age peaks and age peak clusters, presents revised peak clusters based on a greater number of ages and new statistical analysis of data, discusses both granitoid and detrital ages (from both modern and ancient sediments) in terms of the supercontinent cycle, and presents a new comprehensive estimate for the preservation rate of continental crust with time.

2. Monte Carlo kernel density estimation

Estimating probability density from sample data is a fundamental problem in many fields that has been approached with a variety of methods (e.g., Silverman, 1986; Brandon, 1996; Chaudhuri and Marron, 1999, 2000; McLachlan and Peel, 2000; Rudge, 2008). The basic challenge is to estimate the unknown probability density of a random variable (here, the probability of occurrence for an isotopic date of a particular age range) given a finite sample (a finite set of realizations of the random variable). This estimation process is subject to data errors and commonly unknown sampling biases. Here, age errors in the samples reflect uncertainties in individual U/Pb ages arising from measurement uncertainties (e.g., Chang et al., 2006), and the sampling bias reflects non-uniform geological exposure, preservation, and collection. An additional source of uncertainly can arise from sparse sampling in particular data sets or within particular age ranges. Once a density function is estimated, it is important to assess its characteristics in a statistically meaningful way, which is sometimes referred to as the problem of feature significance (Rudge, 2008). Key features in the context of age studies are the time localization, significance, and precise location of peaks and troughs in age spectra.

A key parameter in any distribution estimation is the bandwidth, which is the width of time averaging in the estimation algorithm (Silverman, 1986). A short bandwidth will typically produce numerous low-confidence peaks (i.e., the estimate is under-smoothed), while a long bandwidth will not resolve shorter time features that may be significant (i.e., the estimate is over-smoothed). In this sense, the bandwidth choice and the methodology of implementation can be generally viewed as a regularization process applied to the inverse problem of estimating a density function from sample data (e.g., Aster et al., 2004). In its most basic implementation, kernel analysis estimates are obtained by convolving the age sample distribution, parameterized as a superposition of delta functions, with a kernel function (chosen to be Gaussian). The use of delta functions for characterizing sample age determinations is appropriate if individual age errors are small relative to width of this convolving kernel. The bandwidth of the estimate in this case can be generically specified in terms of the standard deviation for the normal convolving kernel.

Because the bandwidth is typically an ad hoc parameter that is difficult to constrain in advance, a reasonable way to explore regularization tradeoffs is to estimate the unknown distribution using a range of convolving kernel bandwidths and assess feature significance as a function of bandwidth. One example of this general approach is the SiZer (Significant Zero crossings of the derivative) method of Chaudhuri and Marron (1999), which approximates slopes in distribution estimates evaluated for a range of bandwidths to determine significant peaks. Alternatively, optimal bandwidths may be estimated from the data for specific (e.g., Gaussian) kernel types (e.g., Brandon, 1996). In this study we evaluate estimates calculated by the convolution approach for Gaussian kernels corresponding across a scale range of (3σ) bandwidths, w (i.e., the $\pm 1\sigma$ width of the applied Gaussian function is $2w/3$).

Individual sample age errors from isotopic datasets are not necessarily small relative to kernel bandwidths of interest (the mean age error standard deviation for the complete dataset examined here is 18.7 My). We thus incorporate the effect of data and errors into our probability density estimates using a Monte Carlo approach, where each U/Pb age in an n-sample data set is modeled as a statistically independent normally distributed random variable specified by its age estimate and standard deviation. This approach age-widens the influence of each sample into a standard deviation-consistent Gaussian function.

To incorporate Monte Carlo methods into the probability density analysis, we generate M independent realizations of the data set by selecting n individual sample age estimates from the dataset, choosing M to be a large enough number (e.g., 1000) to adequately characterize the associated statistical variation in the kernel density estimate of the probably density for the dataset. During this realization process, we bootstrap resample the data (with replacement) using a random index drawn from an independent uniform distribution to incorporate the influence of finite sampling. This random index approach has a negligible effect on densely sampled age regions, but will decrease the certainty of features associated with small numbers of samples in isolated age regions. As an end-member example, this reduces the effect of a single age-isolated sample from producing a significant peak.

Performing this procedure for a range of kernel bandwidth (i.e., applying multi-scale analysis) we produce a bandwidth-dependent suite of probabilistic kernel density function estimates, with mean and standard deviation envelopes calculated from the underlying M realizations. These realizations reflect the uncertainties of the constituent age data, small sampling effects, and the smoothing effects of the particular Gaussian convolving kernel.

A more general feature of these bootstrapped Monte Carlo probability density function estimates is that probabilistic assessments of feature significance, such as the time localization and significance of peaks, can also be readily estimated from the population of M realizations. For example, given a kernel bandwidth w, the probability of a peak occurring within a particular time interval (as defined by its estimated value being significantly above those of adjoining time intervals within a time region of width w) can be assessed from the M-normalized proportion of times that the count within that region exceeds that of its neighbors. In this evaluation, we utilize a peak detection algorithm successively applied to each of the M realizations. We use the Matlab *findpeaks* function, which is summarized in Appendix 2 with an example. This procedure produces a statistical confidence measure for the reliability of a peak as a function of bandwidth that is consistent with the statistical data assumptions that the individual sample dates are normally distributed and independent. This peak detection algorithm has the desirable feature that it provides a local feature significance measure that is unaffected by sample density variations with age across large data sets. Error bars on peak time estimates determined by this method are estimated by least-squares fitting of a Gaussian function to the kernel-smoothed peak detection region and evaluating its standard deviation.

Multi-scale kernel density analysis of the complete zircon database (37,830 samples) discussed in this paper is shown in Fig. 1 for 3σ Gaussian kernel widths between 1 and 100 My. Fig. 1a shows Monte Carlo bootstrapped estimates of sample counts (log color scale) as a function of Gaussian kernel bandwidth (w). The general trend, not surprisingly, is for numerous short-time-scale features to be resolved at small w and for a few long-time-scale features to be resolved at large w. Fig. 1b shows peak detection confidence results, similarly plotted. Three representative age spectra ($w = 10$, 30 and 90 My) are shown in Fig. 2.

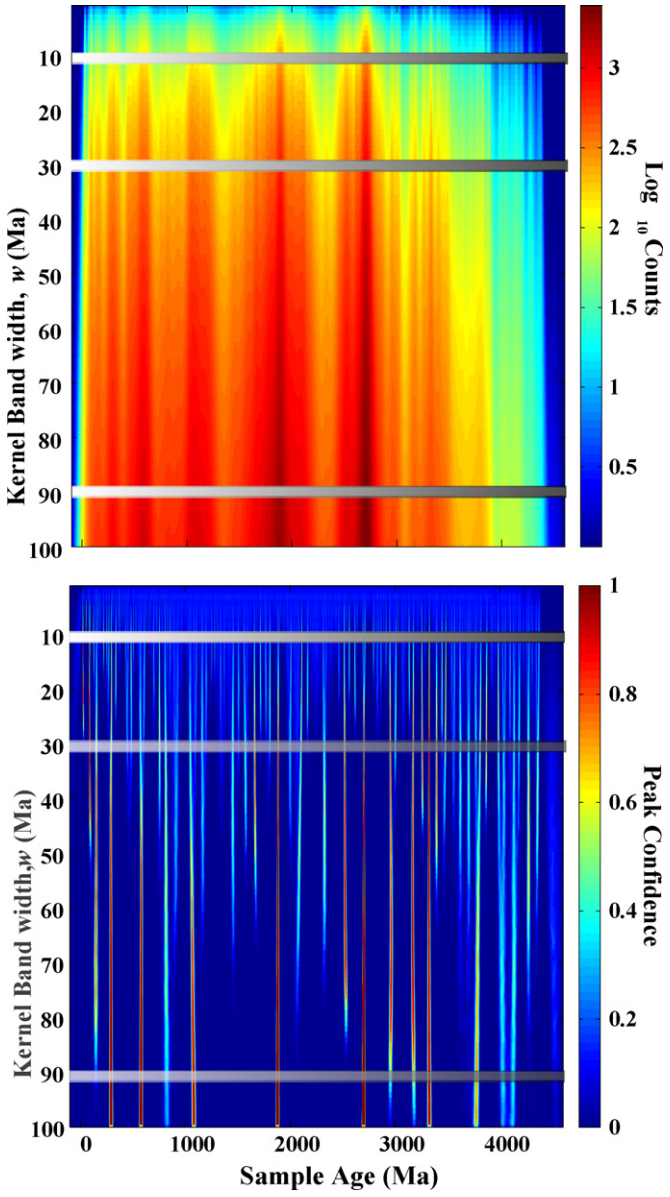

Fig. 1. (a) Monte Carlo mean kernel density estimate (log counts) of complete zircon data set as a function of kernel bandwidth, w (3σ Gaussian kernel bandwidth). Note the resolution of narrow peaks for small bandwidths and of broad, but robust peaks for large bandwidths. Grey lines are cross-sections for density estimates given in Fig. 2. (b) Peak detection confidence (c, see text) for the density determinations of Fig. 1a as a function of w. The three grey bands correspond to representative kernel density determinations shown in Fig. 2.

The age distributions in Fig. 2 display resolution using a constant kernel bandwidth. However, the full feature structure of such data sets, where the optimal bandwidth for feature recognition may vary with position in the age spectrum, can be more comprehensively examined by a multi-scale approach. The peak detection plot of Fig. 1b is shown as a perspective surface in Fig. 3a. Tracking individual peaks as a function of bandwidth from 1 to 100 My in steps of 1 My, we tabulate confidence maxima for constituent peaks at the smallest bandwidth where confidence is maximized. Resulting multi-scale peak determinations are tabulated in the figure. Similar perspective plots and peak age determinations with confidence maxima exceeding 0.68 are shown for detrital ages from modern river sediments, ancient detrital sediments, and orogenic granitoids in Fig. 3b–d, respectively.

Before discussing the U/Pb isotopic age distributions of zircons from orogenic granitoids, it is important to point out that regional variations exist in peak height and peak geographic distribution. For example, the 2.7 Ga peak is commonly assumed to be global in extent, but as pointed out by Condie et al. (2009a), it is characterized in some data sets as resolvable multiple peaks between 2800 and 2600 Ma. The Superior province in Canada strongly contributes to the 2.7 Ga peak. If samples with 2.7 Ga ages from this craton are removed from the age spectrum, the 2.7 Ga peak disappears and two adjacent peaks near 2685 and 2714 Ma become apparent (Fig. 4). The 2685 Ma peak is largely controlled by samples from SW Australia and the 2714 Ma peak by samples from the western Superior province and from Karelia. Another example of geographic bias is the 1870 Ma peak, which is largely controlled by data from Laurentian orogens. Thus, the relative height and other features of an age peak may be controlled by the sampling density in a specific geographic region (or regions), and are not necessarily correlated to the total geographic area represented by the peak on the continents.

3. The orogenic granitoid age spectrum

Monte Carlo simulated age distribution estimates of orogenic granitoids show numerous well-defined peaks that can be statistically characterized for significance (Fig. 3d). In contrast, it is important to be wary of over-interpretation of straightforward age distribution estimates, which may show significant numbers of spurious and questionable (low confidence) peaks (Condie et al., 2009a—hereafter referred to as GR9). We divide the data into 22 cratons or orogens for which there are 40 peaks with confidence levels $c \geq 0.9$ with bandwidths near 30 (Appendix 3). When all of the granitoid data are grouped together, only 20 peaks have $c \geq 0.9$ in multi-scale analysis (Fig. 3d). Of the eight peaks that occur on five or more cratons or orogens (750, 850, 1760, 1870, 2100, 2650, 2700, and 2930 Ma), only three have counterparts in the density probability age spectrum reported in GR9 (1870, 2100, and 2700 Ma). We find seven more peaks that occur on four cratons or orogens (1030, 1700, 2040, 2450, 2600, 2680, and 2880 Ma), of which only three (1700, 2600, and 2680 Ma) were identified in the GR9 paper. Thus six peaks (1700, 1870, 2100, 2600, 2680, and 2700 Ma) emerge as significant, regardless of the estimation algorithms used to estimate the age distribution. All of these peaks except the 2680 Ma peak also have $c \geq 0.9$ when all data are analyzed (Fig. 3d).

In contrast to single age peaks, peak clusters are better defined and more widespread on the continents. As summarized in Table 1 and shown in Fig. 5, 10 peak clusters are prominent in the granitoid age spectrum and five of these are also prominent in the detrital zircon ages. With exception of the 2700 Ma cluster, which is widespread on several continents, each of these clusters has a distinct geographic distribution as summarized in Table 1 (Condie,

Table 1
Summary of major orogenic granitoid age clusters from Fig. 5.

Cluster (Ma)	Major locations
200–100	E Asia, W Europe, E and W Laurentia, New Zealand
350–250	E Asia, W Europe, E and W Laurentia, Australia
650–550	Arabian-Nubian shield; East Africa; Laurentia; East Asia
1150–1000	Laurentia; Central and East Africa
1900–1650	Laurentia; Scandinavia
2200–2100	West Africa; Eastern South America
2600–2450	China; India; Antarctica
2750–2650	Widespread
3000–2900	Pilbara & Yilgarn cratons, W Australia
3350–3250	W Australia, S Africa, China

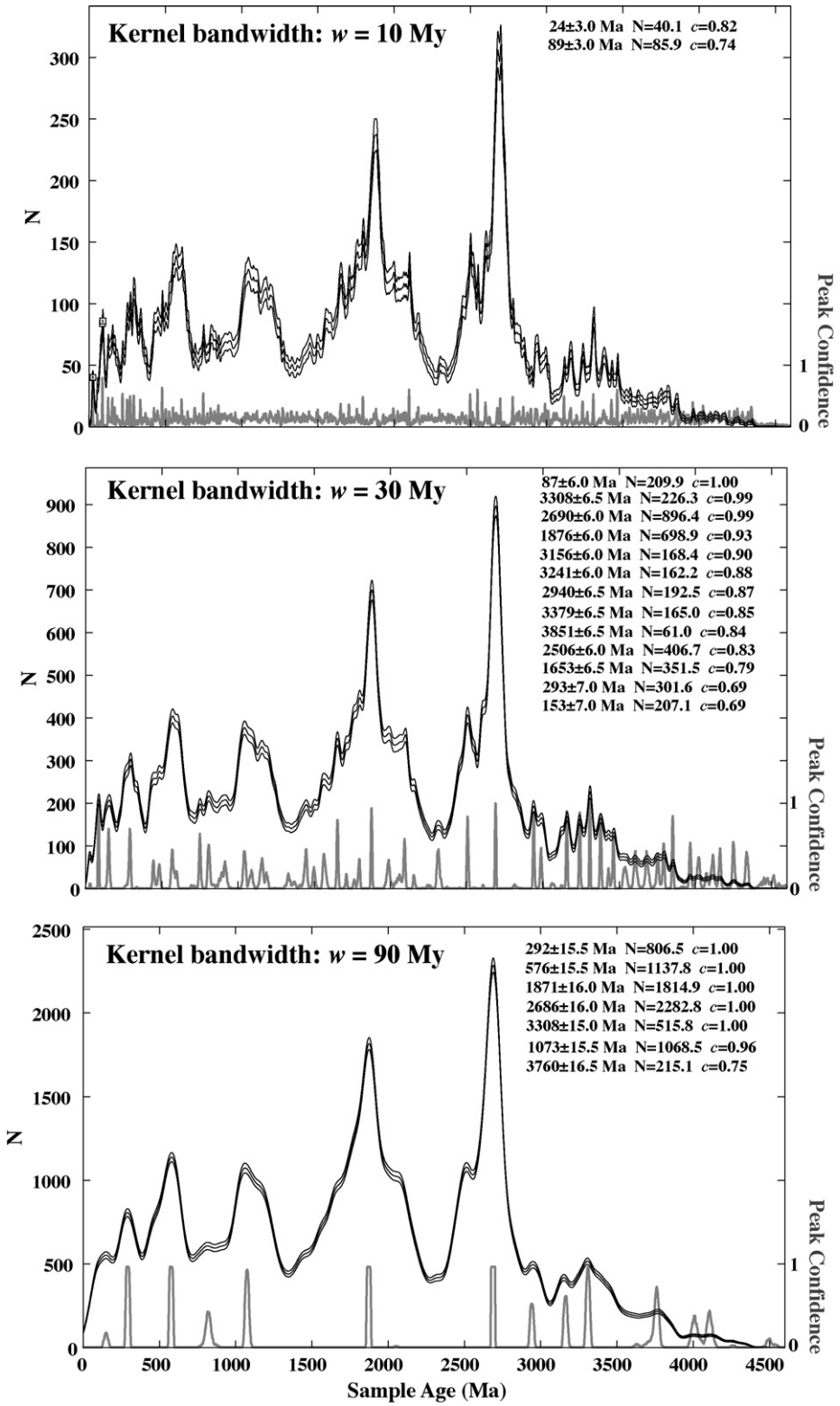

Fig. 2. Three representative kernel density functions for $w = 10, 30$ and 90 My (Fig. 1) with 1σ error envelope. N is representative of the number of samples as a function of age that would be observed in a histogram with bins of width w. Age values for peaks with $c \geq 0.68$ and corresponding 1σ errors are shown at right. Peak age errors are estimated by fitting a Gaussian pulse to the corresponding peak confidence function, c (shown in grey) and reporting the corresponding 1σ points (see text).

1993; Rino et al., 2008; Condie et al., 2009a). In addition to peak clusters, there are two prominent minima in the Precambrian age spectrum: one around 950 Ma and one at 2400–2200 Ma (Fig. 5). The only orogenic granitoids with reported ages between 950 and 900 Ma occur in Svalbaard and Western China (Condie et al., 2009a), but the lateral extent of rocks of this age is unknown. Condie et al. (2009b) suggest that a widespread gap in granitoid ages at 2400–2200 Ma may not be the result of sampling bias, but indicates a decrease in the frequency of global magmatic activity during this time interval.

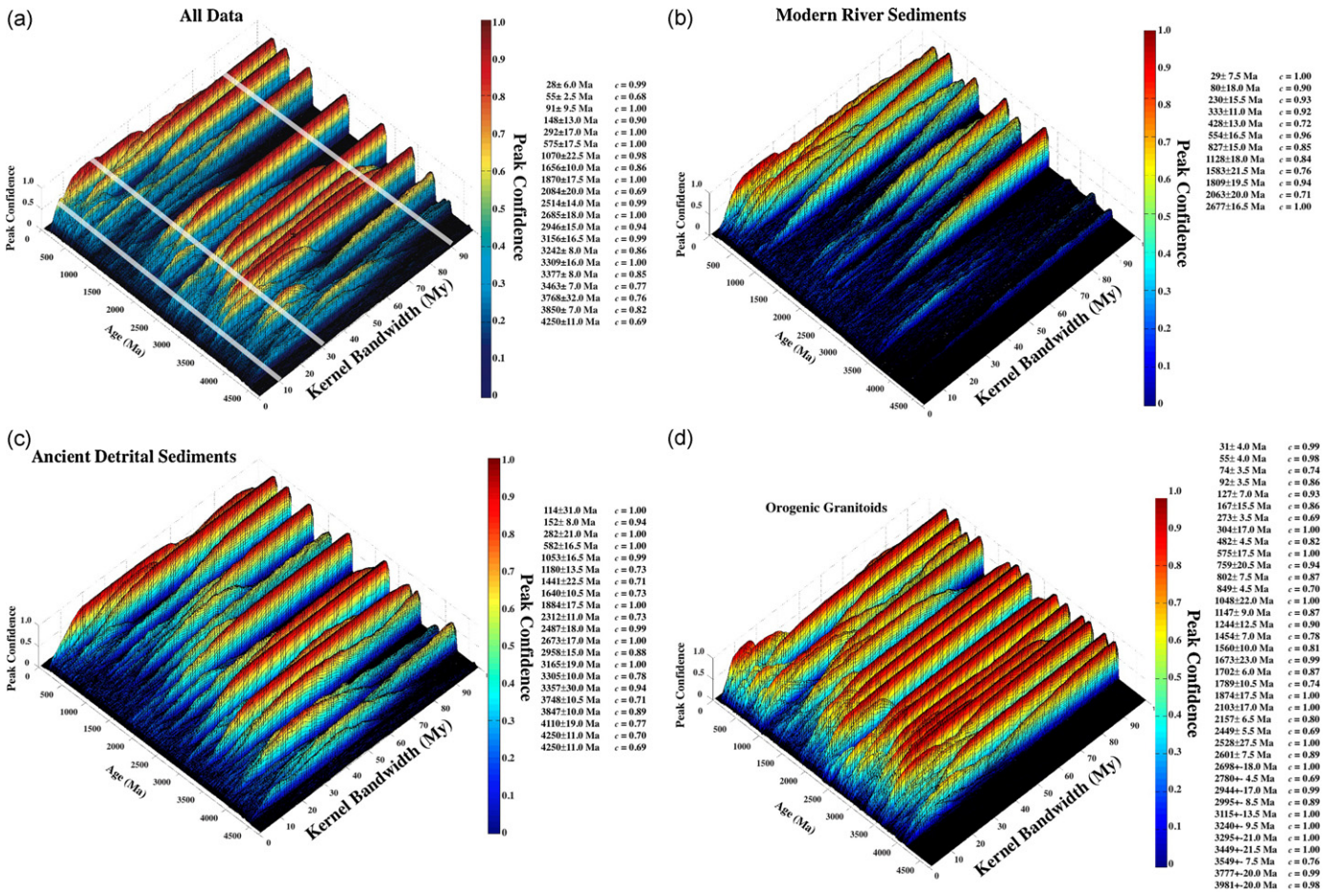

Fig. 3. Peak detection confidence surface (Fig. 1b) shown as a perspective plot. Multi-scale resolution of peaks is accomplished by finding the minimum kernel bandwidth that maximizes the peak confidence for each age ridge that has a peak $c \geq 0.68$ (ages and c values reported at right). (a) All data, (b) detrital zircons from modern rivers, (c) detrital zircons from ancient sedimentary rocks, and (d) zircons from orogenic granitoids. Grey lines in (a) are cross-sections shown in Fig. 2. Other information given in Fig. 2.

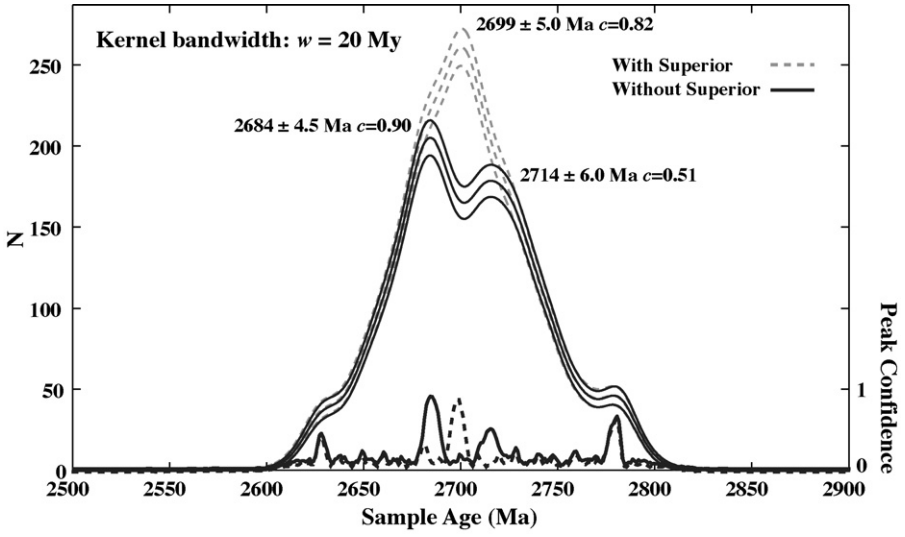

Fig. 4. Orogenic granitoid age spectrum from 2800 to 2600 Ma with and without data from the Superior province, demonstration bifurcation of the 2700 Ma peak when Superior province data are omitted. Other information given in Fig. 2. Data are given in Appendix 2.

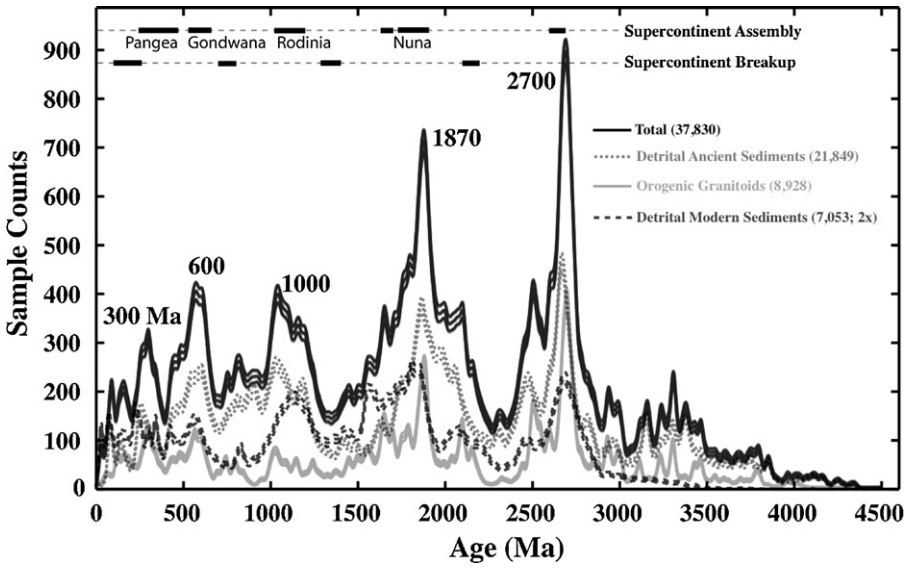

Fig. 5. Estimated distribution of U/Pb zircon ages in orogenic granitoids and detrital zircons for the last 4 Gy with 1σ error envelope. *N* is representative of the number of samples as a function of age that would be observed in a histogram with bins of width 30 My. Data and other information are in Condie et al. (2009a) (spreadsheets updated monthly). The detrital ancient sediment database is multiplied by two for comparative purposes. Approximate central ages for peak clusters are noted. Number of zircon ages: orogenic granitoids, 8928; detrital modern sediments, 6978; detrital ancient sediments, 21,282; total ages, 37,188.

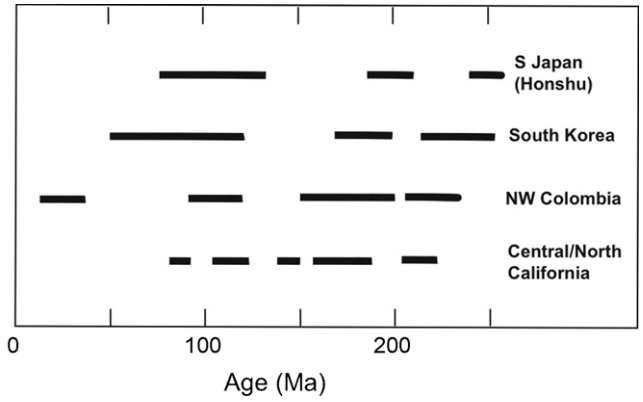

Fig. 6. Episodic subduction-related plutonism around the Pacific basin in the last 250 My. Sources: Nakajima et al. (1990), Aspen et al. (1987), Sagong et al. (2005), Raymond and Swanson (1980) and Lanphere and Reed (1973).

4. Discussion

4.1. Significance of age peaks

Although the episodic nature of orogenic plutonism has been recognized for some time, we still do not know the geographic distribution and cause or causes of such episodicity. The results of this and other recent studies clearly show that age peaks are generally not global in extent, and that most are of only regional or local importance (Rino et al., 2004, 2008; Condie et al., 2009a). The episodic nature of subduction-related magmatism is recognized in young orogens. For instance, in southern Japan, South Korea, northwestern Colombia and central and northern California, three or more episodes of subduction-related granitic plutonism have occurred in the last 250 My (Fig. 6). The episodic nature of such orogenic magmatism has been related to changes in the character or configuration of the converging plate, subduction of buoyant terranes, and variation in sediment supply to trenches (Raymond and Swanson, 1980; Sagong et al., 2005; DeCelles et al., 2009). A recent analysis of Cordilleran orogenic systems suggests that some episodicity may be cyclic on a scale of 25–50 My perhaps related to delamination beneath accreted arcs (DeCelles et al., 2009). Changes in subducting plate character may have acted as a valve turning subduction magmatism on and off at given locations along a subduction system as is spatially evident today (e.g., the Andean system). Since modern plate tectonics has probably been operational at least since the late Archean (Condie and Kroner, 2008; Condie and Pease, 2008; Condie et al., 2009b), it is likely that the age peaks of orogenic plutonism for the last 3 Ga are also related to local changes in the character of converging oceanic plates. This being the case, episodicity of orogenic plutonism reflected by zircon age peaks characterizes subduction systems on a local or regional scale, but it is not characteristic of plutonism on continental or supercontinental scales.

In contrast, clusters of age peaks have greater geographic extent and may retain their identity as more data are added to the age spectrum (Condie et al., 2009a). How representative these age clusters are of the age distribution in past and present continental crust, however, is still a matter of disagreement. Sampling strategies for isotopic dating are generally dictated by mineral exploration, accessibility of outcrops, or availability of geologic maps. None of these necessarily leads to an unbiased representation of the age distribution of the continental crust. For instance, the large age peaks at 2.7 and 1.87 Ga, are strongly influenced by sampling in the Canadian and Baltic shields (Condie et al., 2009a).

One way to address the issue of sampling bias is to consider isotopic ages of detrital zircon populations, which have been reported in large numbers during the last few years (Rino et al., 2008; Condie et al., 2009a). Unlike outcrop sampling, detrital zircon age distributions are controlled by such factors as uplift rate in sediment sources, structural controls of drainage systems, and input from recycled zircons. Detrital sediments may sample sources that have been removed by erosion or sources that are not presently exposed at the surface. One disadvantage of using detrital zircons is that they are not derived exclusively from orogenic granitoids. Although local sources may dominate some detrital populations, an ensemble of detrital ages, including both modern and ancient sediments, should more closely approach the age distribution of continental crust than outcrop sampling alone.

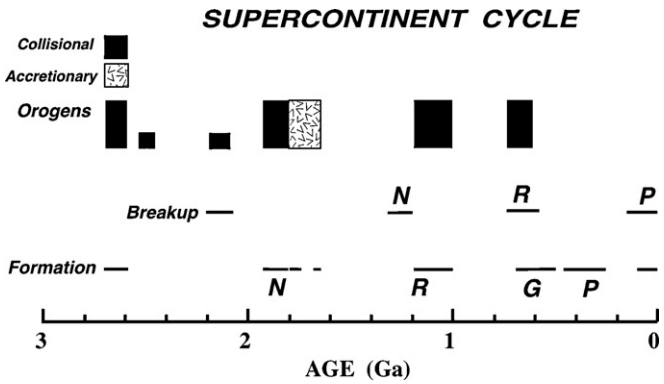

Fig. 7. Relationship of major orogens (collisional and accretionary) to the supercontinent cycle. N, Nuna; R, Rodinia; G, Gondwana; P, Pangea.

4.2. Orogenic granitoids and the supercontinent cycle

Major peak clusters at 2700, 1870, 1100, 600, and 300 Ma occur in all *three* age spectra (granitoid, detrital modern, detrital ancient) as well as in the total age spectrum. The five most prominent age peak clusters shown (Table 1) are closely tied to formation of supercontinents (Fig. 5). This is considered a robust feature because the sampling controls, analytical uncertainties, data processing, and age estimation errors for the granitoid and detrital ages are so very different from each other. Major peak clusters correlate with supercontinent formation and minima may correlate with either supercontinent stasis or the beginning of breakup (Fig. 5). Although there is little supporting evidence for increased production rates of continental crust during supercontinent formation, a recent study by Niu and O'Hara (2009) using incompatible trace elements (esp. Sr and Eu) suggests that some juvenile crust may be produced and preserved in collisional orogens. However, the fact that Nd model ages generally exceed syncollisional granitoid zircon ages by 50–100 My suggests that most juvenile continental crust was produced before major collisions. During supercontinent assembly, the preservation rate of new continental crust may increase due to trapping and isolation in both collisional and accretionary orogens without an increase in actual crustal production rate (Fig. 7).

The first supercontinent (or supercratons) (Bleeker, 2003) appears to have formed at 2700–2650 Ma corresponding to the 2700 Ma age cluster. A second supercontinent (Nuna) formed at 1900–1800 Ma (Zhao et al., 2004; Hou et al., 2008) corresponds to the 1870 Ma age cluster, and a third, Rodinia (Li et al., 2008), corresponds to the 1000 Ma age cluster. Although the formation of Nuna occurred largely between 1900 and 1800 Ma, a large accretionary orogen remained active along an external margin, which housed continued orogenic granitoid activity from 1800 to 1650 Ma (Fig. 7) (Karlstrom et al., 2001). The age cluster at 600 Ma correlates with the growth of Gondwana and the cluster around 300 Ma with the growth of Pangea. Other age clusters may reflect formation of small supercontinents or supercratons. For instance, the age cluster near 2500 Ma may record formation of a small supercraton comprising North China, South India, and part of Antarctica (Zhao et al., 2003). Likewise, the cluster of ages around 2150 Ma may record formation of a supercraton containing West Africa and the eastern part of South America (Zhao et al., 2002; Nomade et al., 2003). It is also possible that an early supercraton formed by collision of the Pilbara and Yilgarn cratons at about 2950 Ma corresponding to the granitoid age cluster at this time (Condie et al., 2009a). If so, these cratons were later rifted apart and re-collided at about 2 Ga forming the Capricorn orogen (Dawson et al., 2002).

During supercontinent breakup, juvenile crust recycling rate may increase, because many of the subduction zones along the leading edges of separating continental fragments may be Andean-type subduction systems, where accretionary prisms are commonly consumed and recycled into the mantle (Kukowski and Oncken, 2006; Scholl and von Huene, 2007; Clift et al., 2009). This process could account for the minima in the orogenic granitoid age spectra during supercontinent stasis or the early stages of breakup (Fig. 5). Previous age minima may record stasis or early breakup of the Late Archean supercontinent(s) at 2200–2100 Ma, the Paleoproterozoic supercontinent Nuna at 1300–1200 Ma, and Rodinia at 750–650 Ma. This correlation breaks down in the last 200 My, where two or three age clusters parallel the breakup of Pangea.

An intriguing feature of the zircon age spectrum is the decrease in supercontinent cycle duration between the first two and second two cycles (830 and 870 My compared to 400 and 300 My, respectively [Figs. 5 and 7]) as illustrated by the major peak clusters. Although this relationship has been previously suggested based on fewer ages (Hoffman, 1997; Bleeker, 2003; Condie, 2004; Campbell and Allen, 2008), the cause is still unknown. Thermal models of Korenaga (2006) suggest that the lithosphere may become more subductable as the mantle cools, so that rates of plate movement may increase with time. In addition or alternatively, recycling of water into the mantle since the Archean may have weakened the mantle and enhanced convection rates (Williams, 2008; Korenaga, 2008), accelerating the supercontinent cycle. Although these hypotheses may not survive as the final explanation, the decrease in duration and change in character of zircon age distributions after 1000 Ma is an intriguing feature that must be accommodated by any model of mantle and lithosphere evolution.

4.3. Continental preservation

Condie (1998) published a histogram showing growth of continental crust with time. Here, continental growth is defined as the volume of continental crust extracted from the mantle minus the amount recycled back into the mantle for a given time interval. Hence, the histogram of continental growth is really a record of *continental crust preservation*, which may or may not be closely correlated the extraction rate of continental crust from the mantle. Armstrong (1981) was first to point out the importance of crustal recycling and emphasized that age peaks in the continental crust are preservational in nature. Condie (1990) also presented a model for Laurentia in which age peaks represent preservation peaks, and more recently Hawkesworth et al. (2009) have suggested preservation may be important. The effect of recycling is very evident on a plot of sediment depositional age versus the average age of detrital zircons contained in sediments (Fig. 8). As with Nd model ages (Miller et al., 1986), the average detrital zircon age increases with decreasing depositional age. What is even more striking is that the rate of recycling increases at 1.8–2.0 Ga, after the first widespread cratons had become established at the end of the Archean and coincident with the formation of perhaps the first large supercontinent (Nuna). This confirms that recycling within the continental crust requires cratons and that uplift related to supercontinent assembly feeds older crust into the erosion cycle.

Nd and Hf isotope data indicate that the major zircon age clusters are times of increased production or/and preservation of juvenile continental crust (Kemp et al., 2006; Condie et al., 2009a; Hawkesworth et al., 2009). Based on new data, it is possible to update the 1998 crustal growth (preservation) graph as shown in Fig. 9. The graph is constructed as described in Condie (1993, 1998) using U/Pb zircon ages (igneous and detrital), whole-rock Nd isotopic data and/or zircon Hf isotopic data, together with geologic maps, from which areal distributions of rocks of known ages are estimated (references in Condie, 1998 and Condie et al., 2009a,b). In contrast to some studies (Rino et al., 2008), we do not use zir-

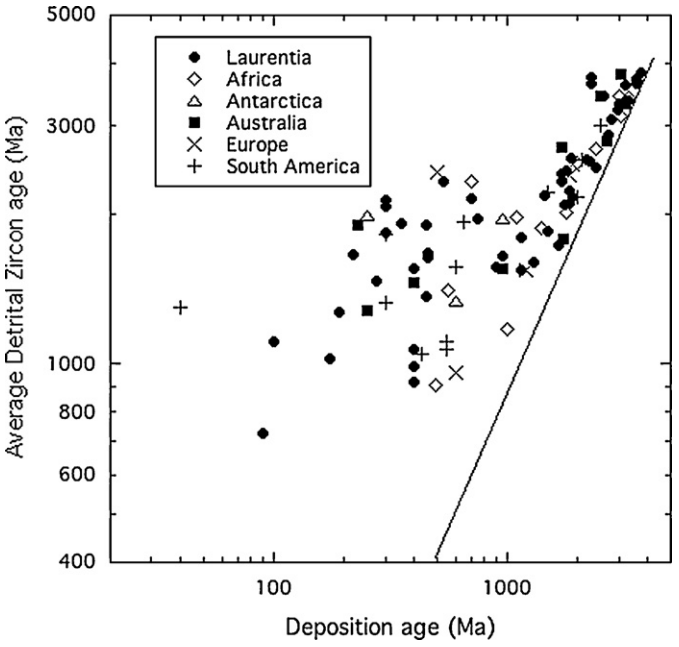

Fig. 8. Graph of average detrital zircon age versus sediment depositional age.

con ages that do not have available Nd or/and Hf isotopic data to estimate the distribution of juvenile continental crust.

The revised juvenile continental growth histogram (Fig. 9) differs from the 1998 version in several ways. First, the peak at about 1200 Ma is smaller indicating that a relatively small volume of new continent was preserved during the Grenville events associated with the formation of Rodinia. Only about 9% of the total continental crust preserved today formed between 1350 and 900 Ma (Condie, 2001) and 7% between 1200 and 1000 Ma. Another difference is the appearance of a cluster at 700–500 Ma, reflecting new U/Pb ages and Nd isotopic data from the Central Asian and Appalachian orogenic belts and other Paleozoic orogenic belts as well as new data from the Arabian-Nubian shield (Stern, 2002; Murphy and Nance, 2002; Jahn, 2004; Jahn et al., 2004; Murphy et al., 2008; Wang et al., 2009a,b; and references therein). The new results suggest that only about 27% of the present continental crust formed during the late Archean (2800–2600 Ma), much less than some previous esti-

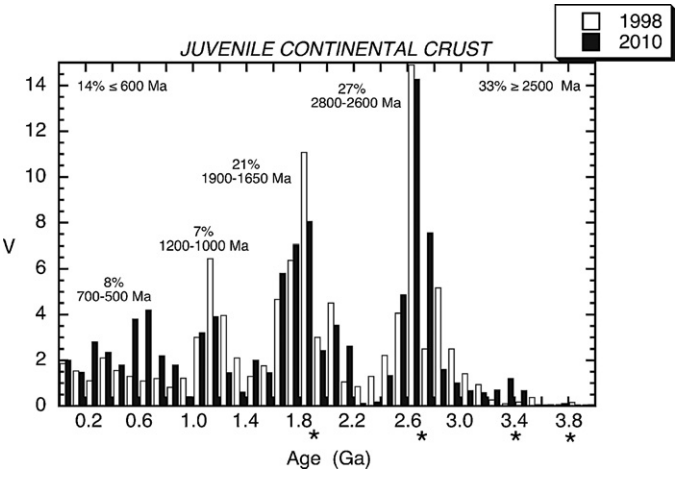

Fig. 9. Distribution of juvenile continental crust in bins of 50 My comparing data from 1998 (Condie, 1998) to data from 2010. Percents are the amounts of juvenile continental crust preserved. Asterisks denote episodes of mafic crust formation based on zircon Hf and oxygen isotope data from zircons (Kemp et al., 2006; Pietranik et al., 2008). Data for the 2010 histogram are given in Appendix 4.

mates (Taylor and McLennan, 1985; Campbell, 2003). However, the rate of growth of Archean crust has varied significantly between continents. For instance, Hf isotope data from zircons suggest that at least 50% of the Laurentian continental crust formed by 2.9 Ga (Wang et al., 2009a,b). Fig. 9 also suggests that about 20% of the continental crust formed during the Paleoproterozoic (1900–1650 Ma). Thereafter, continental growth rates were relatively small: only 7–8% formed during each of the Grenvillian (1200–1000 Ma) and Pan-African events (700–500 Ma). Collectively, about 63% of the preserved continental crust falls into one the four peak clusters in Fig. 9. Approximately one-third of the existing continental crust appears to have formed in the Archean, and only 14% in the last 600 My.

The episodic nature of continental crust preservation is verified by the new data. This also agrees with results from combined Hf and oxygen isotopic data from zircons that suggest episodes in production of juvenile mafic crust at about 2700 and 1900 Ma (Kemp et al., 2006; Pietranik et al., 2008) (Fig. 9). In fact, this mafic crust may have served, at least in part, as a source for the felsic crust produced at these times. Detrital zircon results from Laurentia suggest two major times of juvenile crust production at 2.2–1.6 and 3.4–2.9 Ga (Wang et al., 2009a,b). Although very little crust survives that is older than 3 Ga, Hf isotope data also indicate that 3400 and 3800 Ma were important in terms of mafic crust production (Pietranik et al., 2008).

Another feature of the new crustal growth histogram is verification of a remarkable minimum between 2400 and 2200 Ma. Juvenile granitoids with ages in this time window are reported from only three small geographic areas: the Borborema orogen and Bacaja domain in NE Brazil (Santos et al., 2009; Macambira et al., 2009), the Arrowsmith orogen in western Canada (Hartlaub et al., 2007), and in the Fuping area of China (Zhao et al., 2001). Condie et al. (2009b) discuss the possible significance of this minimum in terms of a widespread shutdown (or slowdown) of planetary magmatism and plate tectonics between 2450 and 2200 Ma.

The supercontinent cycle has been tied to catastrophic events in the mantle, such as collapse of slabs through the 660 km seismic discontinuity and phase transition (Stein and Hofmann, 1994; Tackley et al., 1994; Condie, 2004). However, this is critically dependent upon the Clapeyron slope of the Mg-perovskite reaction, of which recent experimental data suggest that the slope is only slightly negative (Katsura et al., 2003; Fei et al., 2004). This being the case, the perovskite reaction is not likely to support layered convection in a hotter mantle, and thus it is no longer so attractive as a mechanism for catastrophic mantle slab avalanches in the mantle. Hence, the episodicity of age clusters in orogenic granitoids may be related chiefly to the supercontinent cycle, and thus be a robust feature of planets with plate tectonics.

5. Conclusions

Kernel density analysis of orogenic granitic zircon ages and detrital zircon ages suggest that optimum bin width for major age peak identification is 25–30 My. Our results also indicate that the height of age peaks is controlled in part by uneven geographic sampling density, and thus not necessarily correlated to the total geographic area represented by a given age peak on the continents. Six peaks are considered highly significant (1700, 1870, 2100, 2600, 2680, and 2700 Ma), essentially independent of the type of kernel density analysis or bin width used to create the age spectrum. In contrast to single age peaks, clusters of peaks are better defined and have larger geographic distributions. Although ten peak clusters are prominent, only the 2700 Ma cluster is widespread on the continents.

Episodicity of orogenic plutonism as reflected by zircon age peaks characterizes subduction systems on a local or regional scale,

but not on continental or supercontinental scales. In contrast, clusters of ages including data from detrital zircon populations appear to be more representative of widespread continental crust than do ages of single peaks. Clusters of ages at about 2700, 1870 1000, 600, and 300 Ma are represented in both granitoid and detrital zircon populations, a feature that is considered robust since sampling controls, analytical uncertainties, data processing, zircon provenance, and age estimation errors are so very different for each of these sample populations. These age clusters appear to be closely related to supercontinent formation, and intervening age minima show a strong correlation with supercontinent stasis or early stages of breakup.

Peaks in juvenile continental crust growth, as tracked with Nd and Hf isotope data, are likely related to selective preservation in orogens accompanying supercontinent assembly, although continental crustal production rate may also be enhanced during collisions. Decreasing amounts of continental crust formed in the late Archean (27%), the Paleoproterozoic (21%) and the Neoproterozoic–Paleozoic (15%). Approximately one-third of the existing continental crust appears to have formed in the Archean, much less than many previous estimates, and only 14% has formed in the last 600 My.

Appendix A. Supplementary data

Supplementary data associated with this article can be found, in the online version, at doi:10.1016/j.precamres.2010.03.008.

References

Armstrong, R.L., 1981. Radiogenic isotopes: the case for crustal recycling on a near-steady-state no-continental growth Earth. Philosophical Transactions Royal Society London A301, 443–472.

Aspen, J.A., McCourt, W.J., Brook, M., 1987. Geometrical control of subduction-related magmatism: the Mesozoic and Cenozoic plutonic history of Western Colombia. Journal of the Geological Society of London 144, 893–905.

Aster, R., Borchers, B., Thurber, C., 2004. Parameter Estimation and Inverse Problems. Elsevier Academic Press.

Bleeker, W., 2003. The late Archean record: a puzzle in ca. 35 pieces. Lithos 71, 99–134.

Brandon, M., 1996. Probability density plot for fission-track grain-age samples. Radiation Measurements 26 (5), 663–676.

Campbell, I.H., 2003. Constraints on continental growth models from Nb/U ratios in the 3.5 Ga Barberton and other Archean basalt-komatiite suites. American Journal of Science 303, 319–351.

Campbell, I.H., Allen, 2008. Formation of supercontinents linked to increases in atmospheric oxygen. Nature Geoscience 1, 554–558.

Clift, P., Schouten, H., Vannucchi, P., 2009. Arc-continent collisions, sediment recycling and the maintenance of the continental crust. Geology Society London, Spec. Publ. 318, 75–103.

Chang, Z., Vervoort, J., McClelland, W., Knaack, C., 2006. LA_ICP-MS U-Pb dating of zircons: error assessment. Geochimica et Cosmochimica Acta 70, A96.

Chaudhuri, P., Marron, J., 1999. SiZer for exporation of structures in curves. Journal of American Statistical Association 94, 807–823.

Chaudhuri, P., Marron, J., 2000. Scale space view of curve estimation. Annals of Statistics 28, 408–428.

Condie, K.C., 1990. Growth and accretion of continental crust: inferences based on Laurentia. Chemical Geology 83, 183–194.

Condie, K.C., 1993. Chemical composition and evolution of the upper continental crust: contrasting results from surface samples and shales. Chemical Geology 104, 1–37.

Condie, K.C., 1998. Episodic continental growth and supercontinents: a mantle avalanche connection? Earth & Planetary Science Letters 163, 97–108.

Condie, K.C., 2001. Continental growth during formation of Rodinia at 1.35–0.9 Ga. Gondwana Research 4, 5–16.

Condie, K.C., 2004. Supercontinents and superplume events: distinguishing signals in the geologic record. Physics of Earth and Planetary Interiors 146, 319–332.

Condie, K.C., Pease, V., 2008. When did plate tectonics begin on planet Earth? Geological Society of America Special Paper 440, 294.

Condie, K.C., Kroner, A., 2008. When did plate tectonics begin? Evidence from the geologic record. Geological Society of America Special Paper 440, 281–294.

Condie, K.C., Belousova, E., Griffin, W.L., Sircombe, K.N., 2009a. Granitoid events in space and time: constraints from igneous and detrital zircon age spectra. Gondwana Research 15, 228–242.

Condie, K.C., O'Neill, C.O., Aster, R.C., 2009b. Evidence and implications for a widespread magmatic shut-down for 250 My on Earth. Earth & Planet Science Letter 282, 294–298.

Dawson, G.C., Krapez, B., Fletcher, I.R., McNaughton, N.J., Rasmussen, B., 2002. Did late Paleoproterozoic assembly of proto-Australia involve collision between the Pilbara, Yilgarn and Gawler cratons? Geochronological evidence from the Mount Barren Group in the Albany-Fraser orogen of Western Australia. Precambrian Research 118, 195–220.

DeCelles, P.G., Ducea, M.N., Kapp, P., Zandt, G., 2009. Cyclicity in Cordilleran orogenic systems. Nature Geoscience 2, 251–257, doi:10.1038/NGEO469.

Fei, Y., Orman, J.V., Li, J., van Westrenen, W., Sanloup, C., Minarik, W., Kirose, K., Komabayashi, T., Walter, M., Funakoshi, K., 2004. Experimentally determined postspinel transformation boundary in Mg_2SiO_4 using MgO as an internal pressure standard and its geophysical implications. Journal of Geophysical Research 109, BO2305, doi:10.1029/2003JB002562.

Hartlaub, R.P., Heaman, L.M., Chacko, T., Ashton, K.E., 2007. Circ 2.3-Ga magmatism of the Arrowsmith orogeny, Uranium City Region, Western Churchill craton, Canada. Journal of Geology 115, 181–195.

Hawkesworth, C., Cawood, P., Kemp, T., Storey, C., Dhuime, B., 2009. A matter of preservation. Science 323, 49–50.

Hoffman, P.F., 1997. Tectonic genealogy of North America. In: Van der Pluijm, B.A., Marshak, S. (Eds.), Earth Structure: An Introduction to Structural Geology and Tectonics. McGraw-Hill, New York, pp. 459–464.

Hou, G., Santosh, M., Qian, X., Lister, G.S., Li, J., 2008. Configuration of the late Paleoproterozoic supercontinent Columbia: insights from radiating mafic dyke swarms. Gondwana Research 14, 395–409.

Jahn, B.M., 2004. The Central Asian Orogenic Belt and growth of the continental crust in the Phanerozoic. Geological Society of London 226, 73–100, Special Publication.

Jahn, B.M., Capdevilla, R., Liu, D., Vernon, A., Badarch, G., 2004. Sources of Phanerozoic granitoids in the transect Bayanhongor-Ulaan Baatar, Mongolia: geochemical and Nd isotopic evidence, and implications for Phanerozoic crustal growth. Journal of Asian Earth Sciences 23, 629–653.

Karlstrom, K.E., Harlan, S.S., Ahall, K.I., Williams, M.L., McLelland, J., Geissman, J.W., 2001. Long-lived convergent orogen in southern Laurentia, its extensions to Australia and Baltica, and implications for refining Rodinia. Precambrian Research 111, 5–30.

Katsura, T., et al., 2003. Post-spinel transition in Mg_2SiO_4 determined by high P-T in situ X-ray diffractometry. Physics of Earth and Planetary Interiors 136, 11–24.

Kemp, A.I.S., Hawkesworth, C.J., Paterson, B.A., Kinny, P.D., 2006. Episodic growth of the Gondwana supercontinent from hafnium and oxygen isotopes in zircon. Nature 439 (2), 581–583.

Korenaga, J., 2006. Archean geodynamics and the thermal evolution of Earth. American Geophysics Union Monograph 164, 7–32.

Korenaga, J., 2008. Plate tectonics, flood basalts and the evolution of Earth's oceans. Terra Nova 20, 419–439.

Kukowski, N., Oncken, O., 2006. Subduction erosion–the "normal" mode of fore-arc material transfer along the Chilean margin. In: Oncken, O., Chong, G., Franz, G., Giese, P., Gotze, H.-J., Ramos, V.A., Strecker, M.R., Wigger, P. (Eds.), The Andes Active Subduction Orogeny. Springer, Berlin, Chapt. 10.

Lanphere, M.A., Reed, B.L., 1973. Timing of Mesozoic and Cenozoic plutonic events in Circum-Pacific North America. Geological Society of America Bulletin 84, 3773–3782.

Li, Z.X., et al., 2008. Assembly, configuration, and break-up history of Rodinia: a synthesis. Precambrian Research 160, 179–210.

McLachlan, G.J., Peel, D., 2000. Finite Mixture Models. Wiley, New York.

Macambira, M.J.B., Vasquez, M.L., da Silva, D.C.C., Galarza, M.A., de Mesquita Barros, C.E., de Freitas Camelo, J., 2009. Crustal growth of the central-eastern Paleoproterozoic domain, SW Amazonian craton: juvenile accretion vs reworking. Journal of South American Earth Sciences 27, 235–246.

Miller, R.G., O'Nions, R.K., Hamilton, P.J., Welin, E., 1986. Crustal residence ages of clastic sediment, orogeny and continental evolution. Chemical Geology 57, 87–99.

Murphy, J.B., Nance, R.D., 2002. Sm-Nd isotopic systematics as tectonic tracers: an example from West Avalonia in the Canadian Appalachians. Earth-Science Reviews 59, 77–100.

Murphy, J.B., Gutierrez-Alonso, G., Fernandez-Suarez, J., Braid, J.A., 2008. Probing crustal and mantle lithosphere origin through Ordovician volcanic rocks along the Iberian passive margin of Gondwana. Tectonophysics 461, 166–180.

Nakajima, T., Shirahase, T., Shibata, K., 1990. Along-arc lateral variation of Rb-Sr and K-Ar ages of Cretaceous granitic rocks in SW Japan. Contributions to Mineralogy and Petrology 104, 381–389.

Niu, Y., O'Hara, M.J., 2009. MORB mantle hosts the missing Eu (Sr, Nb, Ta and Ti) in the continental crust: new perspectives on crustal growth, crust-mantle differentiation and chemical structure of oceanic upper mantle. Lithos 112, 1–17.

Nomade, S., Chen, Y., Pouclet, A., Feraud, G., Theveniaut, H., Daouda, B.Y., Vidal, M., Rigolet, C., 2003. The Guiana and the West African shield Paleoproterozoic grouping: new Paleomagnetic data for French Guiana and the Ivory Coast. Geophysical Journal International 154, 677–694.

Pietranik, A.B., Hawkesworth, C.J., Storey, C.D., Kemp, A.I.S., Sircombe, K.N., Whitehouse, M.J., Bleeker, W., 2008. Episodic, mafic crust formation from 4.5 to 2.8 Ga: new evidence from detrital zircons, Slave craton, Canada. Geology 36, 875–878.

Raymond, L.A., Swanson, S.E., 1980. Accretion and episodic plutonism. Nature 285, 317–319.

Rino, S., Komiya, T., Windley, B.F., Katayama, I., Motoki, A., Hirata, T., 2004. Major episodic increases of continental crustal growth determined from zircon ages of river sands; implications for mantle overturns in the Early Precambrian. Physics of Earth and Planetary Interiors 146, 369–394.

Rino, S., Kon, Y., Sato, W., Maruyama, S., Santosh, Zhao, D., 2008. The Grenvillian and Pan-African orogens: world's largest orogenies through geologic time, and their implications on the origin of superplume. Gondwana Research 14, 51–72.
Rudge, J.F., 2008. Finding peaks in geochemical distributions: a re-examination of the helium-continental crust correlation. Earth & Planetary Science Letters 274, 179–188.
Sagong, H., Kwon, S.-T., Ree, J-H, 2005. Mesozoic episodic magmatism in South Korea and its tectonic implication. Tectonics 24, doi:10.1029/2004TC001720, TC5002.
Santos, R.J.S., Fetter, A.H., Van Schmus, W.R., Hackspacher, P.C., 2009. Evidence for 2.35 to 2.3 Ga juvenile crust growth in the NW Borborema province, NE Brazil. Geological Society of London 323, 271–281, Special Publication.
Scholl, D.W., von Huene, R., 2007. Crustal recycling at modern subduction zones applied to the past—issues of growth and preservation of continental basement, mantle geochemistry and supercontinent reconstruction. In: Hatcher Jr., R.D., Carlson, M.P., McBride, J.H., Martinez Catalan, J.R. (Eds.), 4D Framework of Continental Crust, 200. Geological Society of America, Memoir, pp. 9–32.
Silverman, B., 1986. Density Estimation. Chapman and Hall, London.
Stein, M., Hofmann, A.W., 1994. Mantle plumes and episodic crustal growth. Nature 372, 63–68.
Stern, R.J., 2002. Crustal evolution in the East African orogen: a Nd isotopic perspective. Journal of African Earth Sciences 34, 109–117.
Tackley, P.J., Stevenson, D.J., Glatzmaier, G.A., Schubert, G., 1994. Effects of an endothermic phase transition at 670 km depth on a spherical model of convection in the earth's mantle. Journal of Geophysical Research 99, 15877–15901.
Taylor, S.R., McLennan, S.M., 1985. The Continental Crust: its composition and evolution. Blackwell Scientific, Oxford, 312 p.
Wang, C.Y., Campbell, I.H., Allen, C.M., Williams, I.S., Eggins, S.M., 2009a. Rate of growth of the preserved North American continental crust: evidence from Hf and O isotopes in Mississippi detrital zircons. Geochimica et Cosmochimica Acta 73, 712–728.
Wang, T., Jahn, B.-M., Kovach, V.P., Tong, Y., Hong, D.-W., Han, B.-F., 2009b. Nd-Sr isotopic mapping of the Chinese Altai and implications for continental growth in the Central Asian Orogenic belt. Lithos 110, 359–372.
Williams, Q., 2008. Water, the solid Earth, and the atmosphere: the genesis and effects of a wet surface on a mostly dry planet. In: Schubert, G. (Ed.), Treatise on Geophysics. Elsevier, Amsterdam, Chapt. 9.05.
Yang, J., Gao, S., Chen, C., Tang, Y., Yuan, H., Gong, H., Xie, S., Wang, J., 2009. Episodic crustal growth of North China as revealed by U-Pb age and Hf isotopes of detrital zircons from modern rivers. Geochimica et Cosmochimica Acta 73, 2660–2673.
Zhao, G., Wilde, S.A., Cawood, P.A., Sun, M., 2001. Archean blocks and their boundaries in the North China craton: lithological, geochemical, structural and P-T path constraints and tectonic evolution. Precambrian Research 107, 45–73.
Zhao, G., Sun, M., Wilde, S.A., 2002. Did South America and West Africa marry and divorce or was it a long-lasting relationship? Gondwana Research 5, 591–596.
Zhao, G., Sun, M., Wilde, S.A., 2003. Correlations between the Eastern block of the North China Craton and the South Indian block of the Indian shield: an Archean to Paleoproterozoic link. Precambrian Research 122, 201–233.
Zhao, G., Sun, M., Wilde, S.A., Li, S., 2004. A Paleo-Mesoproterozoic supercontinent: assembly, growth and breakup. Earth-Science Reviews 67, 91–123.